
Fractals and P Systems

Miguel A. Gutiérrez-Naranjo, Mario J. Pérez-Jiménez

Dpto. de Ciencias de la Computación e Inteligencia Artificial
E.T.S. Ingeniería Informática, Universidad de Sevilla
Avda. Reina Mercedes s/n, 41012, Sevilla, España
{magutier, marper}@us.es

Summary. In this paper we show that the massive parallelism, the synchronous application of the rules, and the discrete nature of their computation, among other features, lead us to consider P systems as natural tools for dealing with fractals. Several examples of fractals encoded by P systems are presented and we wonder about using P systems as a new tool for representing and simulating the fractal nature of tumors.

1 Introduction

Philosophy is written in this grand book –I mean universe– which stands continuously open to our gaze, but it cannot be understood unless one first learns to comprehend the language in which it is written. It is written in the language of mathematics, and its characters are triangles, circles and other geometrical figures, without which it is humanly impossible to understand a single word of it; without these, one is wandering about in a dark labyrinth.

Galileo (1623)

“... clouds are not spheres, mountains are not cones, coastlines are not circles, and bark is not smooth, nor does lightning travel in a straight line ...”

B.B. Mandelbrot [21] (1982)

Along centuries, mathematicians have paid attention to the study of regularities. Definitions and theorems have been claimed as general as possible. Sets or functions not sufficiently regular have been treated as individual curiosities or even as mathematical *monsters*. For example, the Peano curve (a curve which *fills* a plane [26]), the middle third Cantor set [6] or the Koch curve¹ [16, 17] are some of these *monsters*.

¹ The middle third Cantor set and the Koch curve will be discussed below.

The seminal work on fractals was presented by Mandelbrot [21] in 1982 and put the basis of the theory to deal with these *monsters*. In a first approach, we can consider that fractal objects exhibit complexity which holds constant under different scales. A *fractal* is a shape made of parts similar to the whole in some way. This self-similarity occurs over an infinite range of scales in pure mathematical structures but over a finite range in many natural objects such as clouds, coastlines or snowflakes.

In the literature, there are many attempts of defining such objects. In [21] Mandelbrot offers the following *tentative* definition of fractal: *A fractal is by definition a set for which the Hausdorff dimension strictly exceeds the topological dimension*. Some years later Mandelbrot proposed a new definition [22]: *A fractal is a shape made of parts similar to the whole in some way*.

Nowadays there is no a definition of fractals which considers *every* case. Instead of a formal definition, a set F is considered a fractal (in informal sense) if it fits into several properties (see [9] and [32]):

- F has a fine structure, i.e., detail on arbitrary many scales.
- F is too irregular to be described in traditional geometrical language, both locally and globally.
- Often F has some form of self-similarity.
- Usually, its *fractal dimension* (defined in some way) is greater than its topological dimension.
- Fractals are obtained by the application of recursive procedures, usually in a simple way. These procedures often consist on a few rules.
- The computational generation of a fractal is discrete. Fractals are usually defined as the limit of an iterative process performed *step by step*.

One of the most interesting aspects of this field is that fractals have not only a mathematical interest. They allows us an approximation to many phenomena of nature. As R.F. Voss points out in [32], Euclidean geometry provides concise accurate descriptions of man-made objects but inappropriate for natural shapes. Self-similarity seems to be one of the fundamental geometrical construction principles in nature.

In many plants and also organs of animals, this has led to fractal branching structures. For example, in a tree the branching structure allows the capture of a maximum amount of sun light by the leaves; the blood vessel system in a lung is similarly branched so that the maximum amount of oxygen can be assimilated (see [27]). Although the self-similarity in these objects is not strict, we can identify the building blocks of the structure.

In many cases we can also find fractal structures in the non-alive world. Mountains, rivers, coastlines, and clouds are other examples. One of the consequences of these fractal features is that it is impossible to assign quantities such as length or surface area to these natural shapes. There cannot be a simple numerical answer to questions as Mandelbrot's famous *How long is the coastline of Britain?* (see [20]). The most appropriate question is *how irregular* or *what is its fractal dimension?*

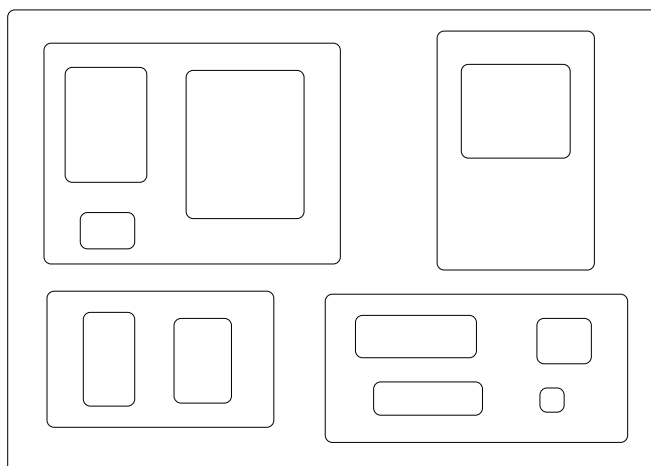


Fig. 1. The membrane structure of a P system

On the other hand, membrane computing is a new non-deterministic model of computation presented by Gh. Păun in [23] which starts from the assumption that the processes taking place in the compartmental structure of a living cell can be interpreted as computations. The devices of this model are called *P systems*.

Roughly speaking, a P system consists of a cell-like membrane structure (see Figure 1) in the compartments of which one places multisets of objects which evolve according to given rules in a synchronous non-deterministic maximally parallel manner².

There exists a *skin* membrane which embraces all the others, separating the system from the environment. The membranes which do not contain other membranes inside are called *elementary membranes*. The regions delimited by the membranes (that is, the space bounded by a membrane and the immediately lower membranes, if there are any) can contain certain objects, that are allowed to be repeated. By means of the application of fixed evolution rules associated with the membranes (or regions), these objects can transform themselves into different ones, and can even go from a region to an adjacent one, crossing the membrane that separates them. Depending on the model, some membranes can be dissolved, divided or created.

The P systems offer two levels of parallelism: on the one hand, the rules within a membrane are applied simultaneously; on the other hand, these operations are performed in parallel in all the membranes of the system.

² A layman-oriented introduction can be found in [25], a formal description in [24], and further bibliography at [33].

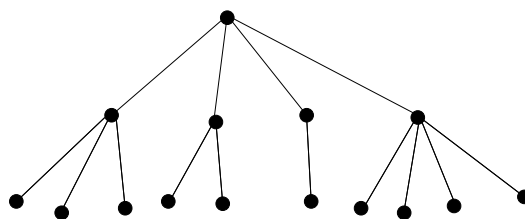


Fig. 2. The membrane structure from Figure 1 as a tree

Each region can be seen as a computing unit (a processor), having its own data (chemical substances) and its local program (given by biochemical reactions). So, the cell can be seen as an unconventional computing device.

To sum up, P systems have the following properties:

- P systems can be considered as structures of nested processors placed in a tree-structure (see Figure 2), i.e., we can consider computations on many scales.
- If we consider P systems where membranes can be dissolved, divided or created, we usually obtain a geometrical shape too irregular to be described in traditional geometrical language, both locally and globally.
- Computations in P systems are obtained by the application of a finite set of rules. The application of these rules allows to obtain a configuration C_{n+1} from another configuration C_n .
- The computation of a P system is discrete, i.e., it is a process performed *step by step*.

In this paper we show that the massive parallelism, the synchronous application of the rules, and the discrete nature of their computation, among other features, lead us to consider P systems as natural tools for dealing with fractals. Several examples of fractals represented by P systems are presented and we wonder about using P systems as a new tool for representing and simulating the fractal nature of tumors.

The paper is organized as follows. First the concept of fractals and P systems with membrane creation are remembered in Sections 2 and 3. In Section 4, two examples of fractals represented by deterministic P systems are presented. In Section 5 we discuss the fractal nature of tumors, how they can be represented by random fractals, and how non-deterministic P systems can deal with random fractals. Finally, some conclusions and lines for future research are given.

2 Fractals

The concept of a *fractal set* is intrinsically linked to the concept of *dimension* (see [9]) and this is not an easy concept to understand. Many greatest mathematicians

like Poincaré, Lebesgue, Brouwer, Cantor or Hilbert, among others, have been involved in the concept of dimension.

At the turn of the 20th century it was one of the major problems in mathematics to determine what dimension means and which properties it has. Mathematically, it is possible to define the dimension of a set in many ways³. Most of these definitions are slight variations of Hausdorff's fundamental definition from 1919, which motivated Mandelbrot's work. As we pointed out in the Introduction, in the seminal paper [21] B.B. Mandelbrot defines a fractal as *a set with Hausdorff dimension strictly greater than its topological dimension*.

A detailed study of the Hausdorff or topological dimensions is out of the scope of this paper. We can start from the usual notion of dimension for which "curves" have dimension 1, "surfaces" dimension 2, and "solids" have dimension 3. Fractal dimension can be considered as a natural extension of this definition.

Let us consider a segment of a given length. If we consider segments $\frac{1}{3}$ of the original length, it is natural to think that we will need 3 new segment to cover the original one. In general, if we consider segments $\frac{1}{r}$ of the original length, we will need $N = r$ segments to cover it.

Let us look at what happens with surfaces. We typically expect that the number of squares needed to cover a surface will increase when smaller boxes are used. For most planar objects, we expect that if squares with side $\frac{1}{3}$ of the original one are used, then the number N of squares needed to cover it will be 3^2 times greater than the number of original squares needed to cover the surface (see Figure 3). If we take a reduction factor $\frac{1}{4}$, the number of squares will be 4^2 times the original one, and in general, if the reduction factor is s then the number of squares needed to cover the surface will be multiplied by $\frac{1}{s^2}$. We recognize the power 2 as the dimension of the object.

Finally, if we consider a solid covered by a set of cubes, we have an analogous reasoning. If we consider new cubes with side $\frac{1}{4}$ of the original one, we will need 4^3 times the number of original cubes. The power 3 is the dimension of the object.

For the line, square, and cube there is a nice power law relation between the number of pieces N and the reduction factor s . This is the law

$$N = \frac{1}{s^D}, \quad (1)$$

where $D = 1$ for the line, $D = 2$ for the square, and $D = 3$ for the cube. In other words, the exponent in the power law agrees exactly with those numbers which are familiar as (topological) dimensions of the line, square, and cube. This intuition for dimension can be extended to *non-integer* dimension.

Derived from the Latin *fractus* meaning *fragmented* (or *frangere*, which mean *to break*), a fractal is a mathematical object with a non-integer⁴ dimension. In

³ C. Tricot did a study of 12 definitions of dimension in [31].

⁴ As pointed out in the Introduction, some *fractals* fall out of this definition, as Peano's curve with dimension 2.0 or the so-called devil's staircase with dimension 1.0 (see, for example, [27]).

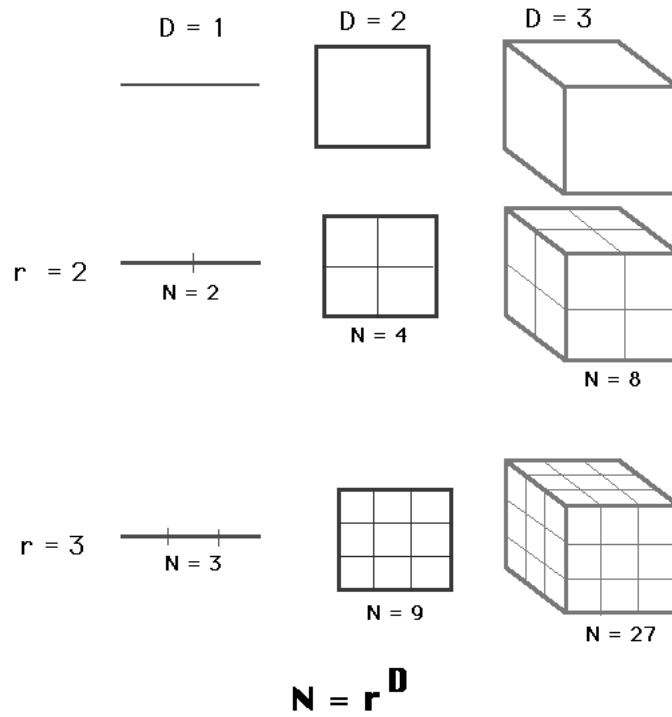


Fig. 3. Intuition for dimension

B.B. Mandelbrot words: *I coined fractal from the Latin adjective fractus. The corresponding Latin verb frangere means “to break”: to create irregular fragments. It is therefore sensible – and how appropriate for our needs! – that, in addition to “fragmented” (as in fraction or refraction), fractus should also mean “irregular”, both meanings being preserved in fragment. [21].*

In Section 4 we will see some examples of fractals and how they can be expressed in terms of membrane computing, but before we will introduce the P system model used in the description.

3 P Systems with Membrane Creation

Since Gh. Păun presented the cellular computation with membranes, many different variants have been proposed. According to the evolution of the membrane structure two big groups can be obtained: P systems where the initial structure does not change along computations and P systems where the tree structure of the membranes vary (or can do it) along computation. The decrease of the number of membranes is made by applying the so-called *dissolution rules*, $[a]_e \rightarrow b$, in

which the object a inside a membrane with label e produces the dissolution of the membrane, a disappears and a new element b and the rest of the multiset in the membrane go to its father (more precisely, they go to the closest non-dissolved ancestor in the membrane hierarchy, since several membranes can dissolve in the same step). Increasing the number of membranes are usually made via *division* of existing membranes or *creating* new ones from objects.

Membranes are created in living cells, for instance, in the process of vesicle mediated transport and in order to keep molecules close to each other to facilitate their reactions. Membranes can also be created in a laboratory (see [19]). Here we abstract the operation of creation of new membranes under the influence of existing chemical substances to define P systems with membrane creation.

Recall that a *P system with membrane creation* is a tuple of the form $\Pi = (O, H, \mu, w_1, \dots, w_m, R)$ where:

1. $m \geq 1$ is the initial degree of the system;
2. O is the alphabet of *objects*;
3. H is a finite set of *labels* for membranes;
4. μ is a *membrane structure* consisting of m membranes labeled (not necessarily in a one-to-one manner) with elements of H ;
5. w_1, \dots, w_m are strings over O , describing the *multisets of objects* placed in the m regions of μ ;
6. R is a finite set of *rules*⁵, of the following forms:
 - a) $[a \rightarrow v]_h$, where $h \in H$, $a \in O$ and v is a string over O describing a multiset of objects. These are *object evolution rules* associated with membranes and depending only on the label of the membrane.
 - b) $a[]_h \rightarrow [b]_h$, where $h \in H$, $a, b \in O$. These are *send-in communication rules*. An object is introduced in the membrane, possibly modified.
 - c) $[a]_h \rightarrow []_h b$, where $h \in H$, $a, b \in O$. These are *send-out communication rules*. An object is sent out of the membrane, possibly modified.
 - d) $[a]_h \rightarrow b$, where $h \in H$, $a, b \in O$. These are *dissolution rules*. In reaction with an object, a membrane is dissolved, while the object specified in the rule can be modified.
 - e) $[a \rightarrow [v]_{h_2}]_{h_1}$, where $h_1, h_2 \in H$, $a \in O$ and v is a string over O describing a multiset of objects. These are *creation rules*. In reaction with an object, a , a new membrane is created. This new membrane is placed inside of the membrane of the object which triggers the rule and has associated an initial multiset v and a label, h_2 .

Rules are applied according to the following principles:

- Rules are used as usual in the framework of membrane computing, that is, in a maximally parallel way. In one step, each object in a membrane can only be

⁵ In this paper we will use a weak version of this model, since we do not use *dissolution* nor *communication* rules, but we want to present the model of *P system with membrane creation* as found in the literature.

used by one rule (non-deterministically chosen when there are several possibilities), but any object which can evolve by a rule of any form must do it (with the restrictions indicated below).

- If a membrane is dissolved, its content (multiset and interior membranes) becomes part of the immediately external one. The skin membrane is never dissolved.
- All the elements which are not involved in any of the operations to be applied remain unchanged.
- The rules associated with the label h are used for all membranes with this label, irrespective of whether or not the membrane is an initial one or it was obtained by creation.
- Several rules can be applied to different objects in the same membrane simultaneously. The exception are the rules of type (d) since a membrane can be dissolved only once.

4 Examples

A fractal set generally contains infinitely many points whose organization is so complicated that it is not possible to describe the set by specifying directly where each point in it lies. Instead, the set may be defined by “the relation between the pieces”. It is rather like describing the solar system by quoting the law of gravitation and stating the initial conditions.

M.F. Barnsley [2]

In this section we present a pair of classic fractals and P systems which can be interpreted as these fractals. They are the *middle third Cantor set* [6] and the *Koch curve* [16, 17]. Following Barnsley, in order to describe the fractal we need to know the initial conditions (or *initial configuration* in terms of membrane computing) and the transformation rules. But we also need other ingredient: as in every computational process, we store the information in some kind of structure data and in order to recognize the data as a *fractal* we need to give an *interpretation* to the data.

We will show below how the data of P systems (objects, labels, membrane structure, etc.) are interpreted, but before we need to fix a technical detail. In the examples we will use the following order between strings of labels. Let H be a set (of labels) and $<$ an order on H . Let us consider $w_1, w_2 \in H^*$ such that w_1 is not a suffix of w_2 and viceversa (consequently, $w_1 \neq w_2$), then we will say that $w_1 <_S w_2$ if and only if there exist $z_1, z_2, w \in H^*$ and $x_1, x_2 \in H$ with $w_1 = z_1 x_2 w$, $w_2 = z_2 x_2 w$ and $x_1 < x_2$.



Fig. 4. First steps for the middle third Cantor set

4.1 The middle third Cantor set

The middle third Cantor set is one of the best known and easiest constructed fractals. It is constructed from a unit interval by a sequence of deletion operations. Let E_0 be the interval $[0, 1]$ of real numbers. Let E_1 be the set of numbers obtained by deleting the middle third of E_0 . In this way the set E_1 consists of two intervals $[0, \frac{1}{3}]$ and $[\frac{2}{3}, 1]$ both of length $\frac{1}{3}$. Deleting the middle third of these intervals we obtain E_2 , i.e., E_2 consists on four intervals $[0, \frac{1}{9}]$, $[\frac{2}{9}, \frac{1}{3}]$, $[\frac{2}{3}, \frac{7}{9}]$, and $[\frac{8}{9}, 1]$ of length $\frac{1}{3^2}$. If we go on with this process, the set E_k consists on 2^k intervals of length $1/3^k$ constructed by deleting the middle third of the intervals from E_{k-1} (see Fig. 4).

The *middle third Cantor set* F consists of the set of elements which belong to E_k , for all k . Formally,

$$F = \bigcap_{k=0}^{\infty} E_k.$$

This set has important mathematical properties. F is an infinite (uncountable) set which consists of the numbers in $[0, 1]$ whose base 3 expansion does not contain the digit 1, i.e., the number which can be expressed as

$$\sum_{k=1}^{\infty} \frac{a_k}{3^k}$$

with $a_k \in \{0, 2\}$ for all $k \geq 1$. Obviously, it is impossible to draw the set F itself with infinitesimal detail, so we only can draw one of the E_k , with a reasonably value of k .

Note also that F , similar to other fractals, *is not* a picture. F is defined as a set of points in the Euclidean space which *admits* a graphical representation with a certain degree of precision. In order to handle F with P systems, we do not think of the graphical representation, but of a computational device which provides the set E_k encoded in a certain way and computes E_{k+1} in the following step.

Such a P system can be easily constructed. Let us consider⁶ the P system $\Pi = (O, H, \mu, w_0, R)$ with $O = \{a, b, c\}$, $H = \{0, 1, 2\}$, $\mu = []_0$, $w_0 = abc$, and R is the set of rules

$$\begin{aligned} [a \rightarrow [abc]_0]_i, & \quad i \in \{0, 2\}, \\ [b \rightarrow [abc]_1]_i, & \quad i \in \{0, 2\}, \\ [c \rightarrow [abc]_2]_i, & \quad i \in \{0, 2\}. \end{aligned}$$

In each configuration, we will consider the elementary membranes, their depth, and for each elementary membrane, the string of labels of the membranes from the elementary membrane to the skin.

- Each elementary membrane will represent a segment of the unit interval.
- The depth of the unitary membrane in the membrane structure will determine the length of the segment represented by the membrane. We will consider that the skin has depth 0 and an elementary membrane at depth k will represent a segment of length $1/3^k$.
- The label of the elementary membrane will determine if the segment is or not considered in the construction of the middle third Cantor set. Segments with label 0 or 2 will be considered. Segments with label 1 will not be considered for the middle third Cantor set (they represent the segments removed).
- Finally, we will use the string of labels of the membranes from the elementary membrane to the skin to order the elementary membranes following the order $<_S$ defined above.

The initial configuration only has the skin and three objects inside $[abc]_0$. We are not interested in the objects placed in the membrane. In fact, along the computation all membranes will be empty, with the exception of the elementary ones, which contains the set abc .

With the interpretation detailed above, this initial configuration C_0 represents a unique segment of length $1/3^0 = 1$. Its label is 0 and this means that the set must be considered. In other words, the initial configuration represents the set E_0 in the construction of the middle third Cantor set.

The P system evolves deterministically, and after the first computation step we obtain the configuration

$$C_1 \equiv [[abc]_0 [abc]_1 [abc]_2]_0.$$

We have three elementary membranes at depth 1 that represents three segments of length $1/3^1$. The order among the strings of labels is $00 <_S 10 <_S 20$ and following the interpretation of the labels, the middle third has label 1 and this means that this segment is not considered. This is the set E_1 in the construction of the middle third Cantor set.

If we give a step more we get the configuration

⁶ The initial degree of the P system is 1, w_0 is the initial multiset of the skin, which has label 0.



Fig. 5. The stage K_1 in the Koch curve

$$C_2 \equiv [[[abc]_0 [abc]_1 [abc]_2]_0 [abc]_1 [[abc]_0 [abc]_1 [abc]_2]_2]_0.$$

This configuration has seven elementary membranes and the order $<_S$ among them is

$$000 <_S 100 <_S 200 <_S 10 <_S 020 <_S 120 <_S 220.$$

The segments represented by the strings 000, 200, 020, and 220 have the length $1/3^2$ and must be considered in the construction of the middle third Cantor set (*as non deleted*). The remaining elementary membranes represent segments which must not be considered (*deleted*): the strings 100 and 120 denote segments of length $1/3^2$ and the string 10 denotes a segment of length $1/3$. With this interpretation, the configuration C_2 can be identified in a natural way with the set E_2 in the construction of the middle third Cantor set.

In each step of computation, the configuration C_k represents the set E_k in the construction of the middle third Cantor set. If we consider the whole computation, in the limit we have a membrane structure with infinite branches. Each of these branches has associated an infinite string of labels composed of 0 and 2. These strings represent the base 3 expansion of the real numbers from the interval $[0, 1]$ which belong to the middle third Cantor set.

4.2 The Koch curve

In 1904, the Swedish mathematician Helge von Koch introduced what is now called the *Koch curve* [16, 17]. As its name expresses, this fractal is a curve and it is also one of the most famous fractals in the literature. This curve has very interesting properties from a mathematical point of view. It has infinite length and it does not admit a tangent to any of its points. This curve has much of the complexity which we can see in nature.

The geometric construction of the Koch curve can be easily described. Let us begin with a straight segment K_0 which we will consider of length one. In a similar way as in the middle third Cantor set, we split K_0 into three segments of length $1/3$. Then we replace the middle third by an equilateral triangle and take away its base (see Figure 5).

Therefore, the next stage on the construction of the Koch curve, K_1 consists of a continuous line composed by four straight segments on length $1/3$. We now repeat the process, taking each of the resulting segments, splitting them into three equal parts and so on. The k -th stage of the construction of the Koch curve consists

on a continuous line composed of 4^k segments of length $1/3^k$. In the limit, we have the Koch curve. If we put together three Koch curves, we have the fractal known as *Koch Snowflake* (see Figure 6).

In a similar way as in the previous example, we present a P system which can be interpreted as the Koch curve. In each step of computation we have an intermediate step of the construction of the Koch curve. Let us consider⁷ the P system $\Pi = (O, H, \mu, w_4, R)$ with $O = \{a, b, c, \alpha, \beta, \gamma\}$, $H = \{1, 2, 3, 4\}$, $\mu = []_4$, $w_0 = \{abc\gamma\}$, and R the following set of 16 rules

$$\begin{aligned} \mathbf{R}_1 &= [\alpha \rightarrow [abc\alpha]_4]_1, & \mathbf{R}_a^i &= [a \rightarrow [abc\alpha]_1]_i, & i &\in \{1, 2, 3, 4\}, \\ \mathbf{R}_2 &= [\beta \rightarrow [abc\beta]_4]_2, & \mathbf{R}_b^i &= [b \rightarrow [abc\beta]_2]_i, & i &\in \{1, 2, 3, 4\}, \\ \mathbf{R}_3 &= [\alpha \rightarrow [abc\alpha]_4]_3, & \mathbf{R}_c^i &= [c \rightarrow [abc\alpha]_3]_i, & i &\in \{1, 2, 3, 4\}, \\ \mathbf{R}_4 &= [\gamma \rightarrow [abc\gamma]_4]_4. \end{aligned}$$

In each configuration, we will consider the elementary membranes, their depth, and for each elementary membrane, the string of labels from the elementary membrane to the skin and the symbol placed in the membrane denoted by a Greek letter α, β , or γ .

- Each elementary membrane will represent a segment.
- The depth of the unitary membrane in the membrane structure will determine the length of the segment represented by the membrane. We will consider that the skin has depth 0 and an elementary membrane at depth k will represent a segment of length $1/3^k$.
- As in the previous example, we will use the string of labels of the membranes from the elementary membrane to the skin to order the elementary membranes following the order $<_S$ defined above.
- Each stage of the construction of the Koch curve consists on a continuous line built with a certain amount of segments, all of them with the same length. If we know the number of such segments and their length, in order to determine exactly an intermediate step of the construction of the Koch curve, the last data that we need is the angle between a segment and the following one. This

⁷ In this case, the initial degree of the P system is also 1 and w_4 is the initial multiset of the skin, which has label 4.



Fig. 6. First steps for the Koch Snowflake

information is given by the symbol α , β , or γ placed inside the elementary membrane.

- If a membrane representing the segment s_1 contains the symbol α , we will consider that the following segment s_2 has a deviation of $\pi/3$ radians with respect to the direction of s_1 .
- If a membrane representing the segment s_1 contains the symbol β , we will consider that the following segment s_2 has a deviation of $-2\pi/3$ radians with respect to the direction of s_1 .
- Finally, if a membrane representing the segment s_1 contains the symbol γ , we will consider that it is the last segment of the line and no other segment is after it.

The initial configuration has only the skin and the objects $abc\gamma$ inside. With the interpretation specified above, this initial configuration C_0 represents a unique segment of length $1/3^0 = 1$. The Greek symbol inside is γ and, coherently, it means that no other segment is after it.

By the application of rules \mathbf{R}_a^4 , $\mathbf{R}_b^4, \mathbf{R}_c^4$, and \mathbf{R}_4 , we obtain the configuration

$$C_1 = [[abc\alpha]_1 [abc\beta]_2 [abc\alpha]_3 [abc\gamma]_4]_4.$$

This configuration has four elementary membranes at depth 1 that represent four segments of length $1/3^1$. The order among the strings of labels is $14 <_S 24 <_S 34 <_S 44$. The first segment (with string 14) contains the symbol α . This means that the second segment (with string 24) has a deviation of $\pi/3$ with respect to the direction of the first one. The second segment contains the symbol β , so we will consider that the third segment has a deviation of $-2\pi/3$ with respect to the second one. Analogously, the fourth segment has a deviation of $\pi/3$ with respect to the third one, since in the third membrane we found the symbol α . Finally, in the last membrane we found the symbol γ to mark the end point.

With this interpretation, the configuration C_1 contains all the necessary information to construct the stage K_1 for building the Koch curve.

The P system is deterministic and if we give a new step, the 16 objects in the configuration C_1 evolve so that in C_2 we have 16 elementary membranes that can be ordered by $<_S$. These membranes represent a continuous line with 16 segments of length $1/3^2$. If we consider the sequence of Greek symbols induced by the order $<_S$ we have

$$\alpha\beta\alpha\alpha\alpha\beta\alpha\beta\alpha\beta\alpha\alpha\alpha\beta\alpha\gamma.$$

Notice that this is exactly the sequence of angles between consecutive segments in the stage K_2 of the construction of the Koch curve.

After j steps, we reach a configuration with 4^j elementary membranes at depth j with a sequence of angles equal to the stage K_j of the Koch curve.

Thus, the above P system encodes all the information needed to build the Koch curve with any precision degree.

4.3 Self-similarity dimension

From the power law (1) in Section 2 we have the relation

$$D = \frac{\log N}{\log \frac{1}{s}}, \quad (2)$$

where N is the number of boxes needed to cover a set and s is the reduction factor. The value D is called the *self-similarity dimension* of the set.

In this way, for curves, a reduction factor of $s = \frac{1}{k}$ leads us to consider $N = k$ boxes, and in this way

$$D = \frac{\log N}{\log \frac{1}{s}} = \frac{\log k}{\log k} = 1.$$

For surfaces, a reduction factor of $s = \frac{1}{k}$ leads us to consider $N = k^2$ boxes, and in this way

$$D = \frac{\log N}{\log \frac{1}{s}} = \frac{\log k^2}{\log k} = \frac{2 \log k}{\log k} = 2.$$

Analogously, for solids

$$D = \frac{\log N}{\log \frac{1}{s}} = \frac{\log k^3}{\log k} = \frac{3 \log k}{\log k} = 3.$$

If we look at the Koch curve, however, the relationship of $N = 4$ to $s = \frac{1}{3}$, $N = 16$ to $s = \frac{1}{9}$ or in general $N = 4^k$ to $s = \frac{1}{3^k}$ is not so obvious. From the self-similarity law we have in this case

$$D = \frac{k \log 4}{k \log 3}.$$

Because $k > 0$, we have that D is a constant

$$D = \frac{\log 4}{\log 3} \approx 1.2619.$$

Hence the power law relation between the number of pieces and the reduction factor gives the same number D , regardless of the scale we use for the evaluation. This value $D = \log 4 / \log 3$ is the self-similarity dimension of the Koch curve. A non-integer dimension.

A similar reasoning leads to estimate the *self-similarity dimension* of the middle third Cantor set, where the stage E_k consists on 2^k intervals of length $1/3^k$. Figure 7 shows the self-similarity dimension of these fractal objects.

5 Applications

As pointed out in the Introduction, one of the most important features of fractals is that they are far from being merely mathematical curiosities or computational

object	scale s	pieces N	dimension D_s
Koch Curve	$1/3^k$	4^k	$\log 4 / \log 3 \approx 1.2619$
Cantor Set	$1/3^k$	2^k	$\log 2 / \log 3 \approx 0.6309$

Fig. 7. Self-similarity dimension

art objects. Fractals are one of the most powerful tools for describing many natural objects both from alive and non-alive world.

Tree branching, blood vessels, clouds, rivers, mountains or coastlines are only some of the examples. Many of the ways in which matter condenses on the microscopic scale seem to generate fractals. Fractals also provide the language and the formalism for studying physical processes (such as diffusion and vibration) on such structures. Diffusion on complex proteins with fractal structures has important biological implications. For physicists, unpredictable changes of any quantity V varying in time t are known as *noise*. The traces made by the noise is a fractal curve and there is a direct relationship between the fractal dimension and the logarithmic slope of the spectral density⁸.

5.1 Tumors and P systems

Maybe one of the most promising applications of fractals is in the study of tumors. An individual tumor cell has the potential, over successive divisions, to develop into a cluster of tumor cells. Further grow and proliferation leads to the development of an avascular tumor consisting of approximately 10^6 cells which feed on oxygen and other nutrients present in the local environment.

The rapid growth and resilience of tumors make it difficult to believe that they behave as disorganized and diffuse cell mass and suggests instead that they are emerging, opportunistic systems. If this hypothesis holds true, the growing tumor and not only the single cell must be investigated and treated as a self-organizing complex dynamic system. This cannot be done with currently available in vitro/in vivo models or common mathematical approaches.

In [12] we proposed a first approach to the simulation and the study of the growth of a tumor by using P systems. In membrane systems a local, modular and topological modeling of biological phenomena is easily achieved. All this features are not easily reached when using other models, like differential equations or cellular automata.

Membrane systems own several interesting features which make them suitable for this study. In particular, P systems treat the discrete nature of actual cells in a realistic manner. Each cell can be seen as an independent computing unit with its own behavior. In this way, a local modeling of the process can be simulated

⁸ For more applications of fractals, see, for example, [8, 5, 32, 27].

and then, the evolution of the whole tumor can be studied as the sum of all local performances together with the network of interactions among the cells.

The model followed in [12] for the study of the growth of tumors was the *spheroid model*. The vast majority of classic models apply specifically to multicell spheroids which have a characteristic structure of a proliferating rim and a necrotic core, separated by a band of quiescent cells.

Over the years, researchers have devised several methods for producing tumor cells aggregated or *spheroids*⁹ that can be used to study tumor invasion in a 3D model system.

Following this model, in the earliest stages of development tumor growth seems to be regulated by direct diffusion of nutrients and wastes from and to surrounding tissue. When a tumor is very small, every cell receives nourishment by simple diffusion and the growth rate is exponential in time. However, this stage cannot be sustained because as a nutrient is consumed its concentration must decrease towards the center of the tumor. The concentration of a vital nutrient at the center will fall below a critical level.

Unfortunately, this is not the end of the process. Indeed, a majority of tumors exhibit the phenomenon of angiogenesis marking the transition from the relatively harmless and localized avascular state described above to the more dangerous vascular state wherein the tumor develops the ability to proliferate, invade surrounding tissue, and metastasize to distant parts of the body.

After the early stages of growth, the avascular spheroids consist structurally of an inner zone of necrotic cells (dead due to lack of nutrients) and an outer zone of living cells. This outer zone can be further divided into a layer largely composed of quiescent cells and a layer largely composed of proliferating cells, although dead cells are also found adjacent to both quiescent and proliferating cells [30]. At this stage the spheroids tend to reach a finite size of at most a few millimeters in diameter [11]. In this state of dynamic equilibrium there is a balance between mitosis and the death and disintegration of tumor cells into waste products, mainly water.

The spheroid model has very nice mathematical properties, but recent studies (see [13, 1, 3, 7, 18, 15, 29, 28] among many others) in the growth of tumors show that the surface of the tumor is far from being a smooth surface. Even more, it seems to be a relation between the fractal dimension of the surface of the tumor and the stages of the disease. In [15], Kikuchi *et al.* point that *the surface of solid components in cystic epithelial ovarian cancers has a fractal structure and the mean fractal dimension may differ according to the stages of the disease and histologic types. Fractal geometry (...) can be used for describing the pathological architecture of ovarian tumors and for yielding insights into the mechanisms of tumor growth.*

These studies show the necessity of going deeper in the relation between fractals and tumors. This study will need new tools for handle information and computing/simulating/predicting results. As pointed by Baish and Jain in [1]: *If carefully*

⁹ The classical schematic representation of the spheroid can be seen in [4] or [14].

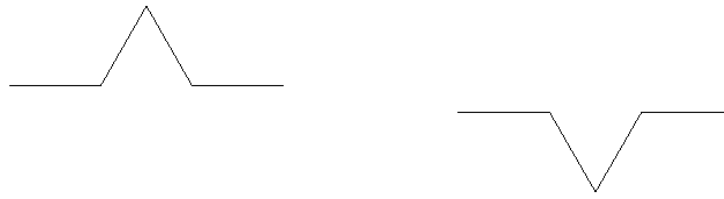


Fig. 8. Two orientations

applied, fractal methods may someday have a significant impact in our understanding of challenges in treatment delivery and diagnosis of cancer.

6 Random Fractals

Self-similar fractals as Koch curve differs from natural fractals in one significant aspect. They are *exactly* self similar, and they cannot be considered as *realistic* models of fractals in nature. The concept of fractal dimension however, can also be applied to such *statistically self-similar* objects. For example, each small section of the coastline looks like (but not exactly like) a larger portion. The property that objects can look statistically similar while at the same time different in detail at different length scales, is the central feature of fractals in nature. The coastline is random in the sense that (unlike the Koch curve) a large scale view is insufficient to predict the exact details of a magnified view. Yet, the way in which the detail varies as one changes length scale is once again characterized by a fractal dimension.

The Koch snowflake are not perceived as a realistic model of a coastline even if we compare it with a real coastline with the same dimension. The reason lies in the lack of randomness. Randomizing a deterministic classical fractal is the first approach generating a realistic natural shape.

For example, the method for including randomness in the Koch snowflake construction requires only a very small modification of the classical construction. A straight line segment will be replaced as before by a broken line of four segments, each one one-third as long as the original segment. However, there are two possible orientations in the replacement step: the small angle may go either to the left or to the right (see Figure 8).

If one of these orientations is chosen in each replacement step, we obtain a *random Koch curve*. Figure 9 shows a random Koch snowflake. Note that this fractal represents a *realistic* shape of a fractal from nature.

In this process some mathematical characteristics of the Koch snowflake will be retained, for example the fractal dimension of the curve will be the same, the area surrounded is finite but the length of the curve is infinite, etc., but the visual appearance is drastically different: it looks much more like the outline of the island or a tumor than the original Koch curve.

6.1 Random fractals and P systems

In Section 4 we present two P systems which encode the Koch curve and the middle third Cantor set with an appropriate interpretation of the objects. Both are deterministic, and in both the configuration C_n can be identified with the n -th stage in the construction of the fractal.

The construction of random fractals with P systems can be performed in a very natural way by using the non-determinism of P systems. For example, in the first step of the construction of the Koch curve we start with a straight line and there are two possible new reachable stages (see Figure 8). Analogously, we can modify the P system presented in Section 4 and obtain a non-deterministic P system such that two possible configurations are reachable from the initial configuration. Each of these configurations can be interpreted as one of the reachable stages in the construction of the Koch curve.

Let us consider the following P system with initial degree 1,

$$\Pi = (O, H, \mu, w_4, R),$$

with $O = \{s, a_r, b_r, c_r, a_l, b_l, c_l, \alpha_r, \beta_r, \alpha_l, \beta_l, \gamma\}$, $H = \{1, 2, 3, 4\}$, $\mu = []_4$, $w_4 = \{s\gamma\}$, and R the following sets of rules

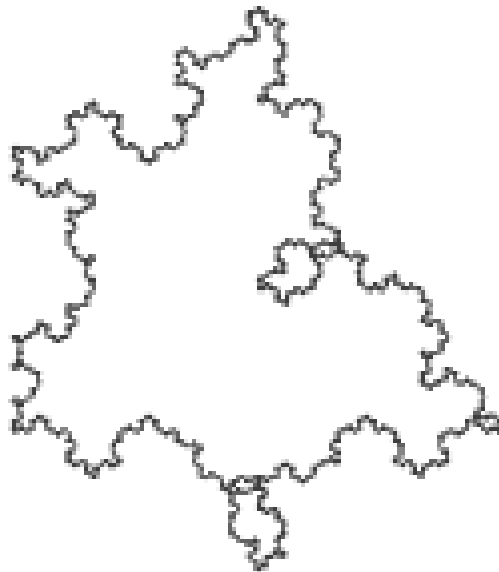


Fig. 9. Random Koch Snowflake

$$\left. \begin{array}{l} [s \rightarrow a_r b_r c_r]_i \\ [s \rightarrow a_l b_l c_l]_i \end{array} \right\} i \in \{1, 2, 3, 4\} \quad \left. \begin{array}{l} [\alpha_j \rightarrow \alpha'_j]_1 \\ [\beta_j \rightarrow \beta'_j]_2 \\ [\alpha_j \rightarrow \alpha'_j]_3 \\ [\gamma \rightarrow \gamma']_4 \end{array} \right\} j \in \{l, r\}$$

$$\left. \begin{array}{l} [a_j \rightarrow [s\alpha_j]_1]_i \\ [b_j \rightarrow [s\beta_j]_2]_i \\ [c_j \rightarrow [s\alpha_j]_3]_i \\ [\gamma' \rightarrow [s\gamma]_4]_4 \end{array} \right\} \begin{array}{l} i \in \{1, 2, 3, 4\} \\ j \in \{l, r\} \end{array} \quad \left. \begin{array}{l} [\alpha'_j \rightarrow [s\alpha_j]_4]_1 \\ [\beta'_j \rightarrow [s\beta_j]_4]_2 \\ [\alpha'_j \rightarrow [s\alpha_j]_4]_3 \end{array} \right\} j \in \{l, r\}$$

In this case, the interpretation of the P system as a fractal is a little more complicated. In the same way as in the deterministic Koch curve, we will consider the elementary membranes, their depth, and for each elementary membrane, the string of labels of the membranes from the elementary membrane to the skin and the special symbol placed in the membrane, taken from the set $\{\alpha_r, \beta_r, \alpha_l, \beta_l, \gamma\}$.

The interpretation of these special symbols is quite natural. In the deterministic case, if a membrane representing the segment s_1 contains the symbol α , we will consider that the next segment s_2 has a deviation of $\pi/3$ radians with respect to the direction of s_1 . In this case, α_r represents a deviation of $\pi/3$ and α_l a deviation of $-\pi/3$. Analogously, in the *deterministic* Koch curve, if a membrane representing the segment s_1 contains the symbol β , we will consider that the next segment s_2 has a deviation of $-2\pi/3$ radians with respect to the direction of s_1 . In this case, β_r represents a deviation of $-2\pi/3$ and β_l a deviation of $2\pi/3$. Finally, if a membrane representing the segment s_1 contains the symbol γ , we will consider that it is the last segment of the line and no other segment is after it.

The main difference consists on that in this P system only configurations in an *even* step will be considered as intermediate stages of the construction of the fractal. Odd steps will be considered as intermediate steps.

The remaining information is stored in a similar way as in the deterministic case:

- Each elementary membrane will be considered a segment.
- The depth of the unitary membrane in the membrane structure will determine the length of the segment represented by the membrane. We will consider that the skin has depth 0 and an elementary membrane at depth k will represent a segment of length $1/3^k$.
- As in the previous example, we will use the string of labels of the membranes from the elementary membrane to the skin to order the elementary membranes following the order $<_S$ defined above.

The initial configuration only has the skin and the objects $s\gamma$ inside. With the interpretation detailed above, this initial configuration C_0 represents a unique segment of length $1/3^0 = 1$. The Greek symbol inside is γ and, coherently, it means that no other segment is after it. This is the stage K_0 in the construction of the Koch curve.

The symbol s can trigger two different rules. One of these rules is chosen in a non-deterministic way. This choice determines the orientation of the next stage in the construction of the Koch curve. Let us suppose that the rule $[s \rightarrow a_r b_r c_r]_4$ is chosen and the configuration $C_1 = [a_r b_r c_r \gamma']_4$ is reached (γ also evolves to γ'). The following step is deterministic and the configuration $C_2 = [[s\alpha_r]_1 [s\beta_r]_2 [s\alpha_r]_3 [s\gamma]_4]_4$ is obtained.

We have four elementary membranes at depth 1 that represents four segments of length $1/3^1$. The order among the strings of labels is $14 <_S 24 <_S 34 <_S 44$. The first segment (with string 14) contains the symbol α_r . This means that the second segment (with string 24) has a deviation of $\pi/3$ with respect the direction of the first one. The second segment contains the symbol β_r , so we will consider that the third segment has a deviation of $-2\pi/3$ with respect to the second one. Analogously, the fourth segment has a deviation of $\pi/3$ with respect to the third one, since in the third membrane we found the symbol α_r . Finally, in the last membrane we found the symbol γ to mark the end point.

This configuration C_2 represents one of the possible stages K_1 in the construction of the random Koch curve.

The next steps in the construction are obtained in a similar way. Every occurrence of the symbol s evolves in a non-deterministic way in the even steps and we obtain a random Koch curve.

7 Conclusions and Future Work

Fractals are nowadays one of the most powerful tools for describe nature in a realistic manner. As Galileo said, we cannot understand nature unless one first learns to comprehend the language in which it is written, but also as Voss pointed out [32], Galileo was wrong in terms of nature's preferred dialect.

In nature, we do not find circles or triangles. We can use circles or triangles in order to approximate in a reasonably way many objects in nature, but if we need a more detailed approximation, we must leave Plato's world.

This is the big contribution (or one of them) by B.B. Mandelbrot. The scientific, philosophical, and artistic consequences of this work are today a vivid discussion field.

Nature is written in fractal language and we need tools for dealing easily with this language. In this paper we present a first work checking whether P systems provide an appropriate tool for handling fractals. On the one hand, the massive parallelism, the synchronous application of the rules, and the discrete nature of their computation, among other features, lead us to consider P systems as natural tools for dealing with fractals. On the other hand, the main drawback is that P systems work with data structures which do not have a *geometrical* intuition, in the sense that concepts as length or angle are not in membrane computing terminology. This leads us to the necessity of giving a geometrical interpretation to the data of the P systems in order to consider it as a fractal.

But being not so close to geometry in the data structure can also be an advantage, since we are not tied to intuition in order to study and discover new properties of fractals.

The main research lines open in this work are, on the one hand, that P systems seem to be a good tool for dealing with fractals and, in the other hand, that medicine, and in particular the tumor growth study needs new tools for dealing with the fractal nature of tumors.

Acknowledgement

This work is supported by project TIN2005-09345-C04-01 of Ministerio de Educación y Ciencia of Spain, cofinanced by FEDER funds.

References

1. J.W. Baish, R.K. Jain: Fractals and cancer. *Cancer Research*, 60 (2000), 3683–3688.
2. M.F. Barnsley: Lecture notes on iterated function systems. *Proceedings of Symposia in Applied Mathematics*, AMS, 39 (1989), 127–144.
3. A. Brú, J.M. Pastor, I. Fernaud, I. Brú, S. Melle, C. Berenguer: Super-rough dynamics on tumor growth. *Physical Review Letters*, 81, 18 (1998), 4008–4011.
4. H.M. Byrne: Modelling avascular tumour growth. In *Cancer Modelling and Simulation* (L. Preziosi, ed.), CRC Press LLC, 2003.
5. A. Bunde, S. Havlin, eds.: *Fractals in Science*. Springer-Verlag, 1995.
6. G. Cantor: *Über unendliche, lineare Punktmannigfaltigkeiten V. Mathematische Annalen*, 21 (1883), 545–591.
7. S.S. Cross: Fractals in pathology. *Journal of Pathology*, 182 (1997), 1–8.
8. M. Dekking, J.L. Véhel, E. Lutton, C. Tricot, eds.: *Fractals: Theory and Applications in Engineering*. Springer-Verlag, 1999.
9. K. Falconer: *Fractal Geometry*. Mathematical Foundations and Applications. John Wiley & Sons, 1990.
10. J. Feder: *Fractals*. Plenum Press, New York, 1988.
11. J. Folkman, M. Hochberg: Self-regulation of growth in three dimensions. *J. Exp. Med.*, 138 (1973), 745–753.
12. M.A. Gutiérrez-Naranjo, M.J. Pérez-Jiménez, F.J. Romero-Campero: Simulating avascular tumours with membrane systems. In *Third Brainstorming Week on Membrane Computing* (M.A. Gutiérrez-Naranjo, A. Riscos-Núñez, F.J. Romero-Campero, D. Sburlan, eds.), RGCN Report 01/2005. Fénix Editora, Sevilla, 2005, 185–195.
13. K.M. Iftekharuddin, W. Jian, R. Marsh: Fractal analysis of tumor in brain MR images. *Machine Vision and Applications*, 13 (2003), 352–362.
14. D.S. Jones, B.D. Sleeman: Growth of tumours. In *Differential Equations and Mathematical Biology*. Chapman & Hall/CRC, 2003.
15. A. Kikuchi, S. Kozuma, K. Sakamaki, M. Sito, G. Marumo, T. Yasugi, Y. Take-tani: Fractal tumor growth of ovarian cancer: Sonographic evaluation. *Gynecologic Oncology*, 87, (2002), 295–302
16. H. von Koch: Sur one courbe continue sans tangente, obtenue par une construction géométrique élémentaire. *Arkiv för Matematik*, 1 (1904), 681–704.

17. H. von Koch: Une méthode géométrique élémentaire pour l'étude de certaines questions de la théorie des courbes planes. *Acta Mathematica*, 30 (1906), 145–174.
18. G. Landini, J.W. Rippin: How important is tumour shape? Quantification of the epithelial-connective tissue interface in oral lesions using local connected fractal dimension analysis. *Journal of Pathology*, 179 (1996), 210–217.
19. P.L. Luisi: The chemical implementation of autopoiesis. In *Self-Production of Supramolecular Structures* (G.R. Fleishaker et al., eds.), Kluwer, Dordrecht, 1994.
20. B.B. Mandelbrot: How long is the coast of Britain? Statistical self-similarity and fractional dimension. *Science*, 155 (1967), 636–638.
21. B.B. Mandelbrot: *The Fractal Geometry of Nature*. W.H. Freeman, New York, 1982.
22. B.B. Mandelbrot: Cited in [10] (p.11) as *Private communication*, 1987.
23. Gh. Păun: Computing with membranes. *Journal of Computer and System Sciences*, 61, 1 (2000), 108–143.
24. Gh. Păun: *Membrane Computing. An Introduction*. Springer-Verlag, Berlin, 2002.
25. Gh. Păun, M.J. Pérez-Jiménez: Recent computing models inspired from biology: DNA and membrane computing. *Theoria*, 18 (2003), 72–84.
26. G. Peano: Sur une courbe, qui remplit toute une aire plane. *Mathematische Annalen*, 36 (1890), 157–160.
27. H.-O. Peitgen, H. Jürgens, D. Saupe: *Fractals for the Classroom*. Springer-Verlag, 1992.
28. A.N dos Reis, J.C.M. Mombach, M. Walter, L.F. de Avila: The interplay between cell adhesion and environment rigidity in the morphology of tumors. *Physica A*, 322 (2003), 546–554.
29. R. Sedivy, S. Thumer, A.C. Budinsky, W.J. Köstler, C.C Zielinski: Short-term rhythmic proliferation of human breast cancer cell lines: Surface effects and fractal growth patterns. *Journal of Pathology*, 197 (2002), 163–169.
30. R.M. Sutherland: Cell and environment interaction in tumour microregions: The multicell spheroid model. *Science*, 240 (1988), 177–184.
31. C. Tricot: Douze définitions de la densité logarithmique. *C.R. Acad. Sci. Paris, Sér. I Math.*, 293 (1981), 549–552.
32. R.F. Voss: Fractals in nature: From characterization to simulation. In *The Science of Fractal Images* (H.-O. Peitgen, D. Saupe, eds.), 1988, 21–70
33. P systems web page: <http://psystems.disco.unimib.it/>